INL/CON-10-19076
PREPRINT

# An Electromotive Force Measurement System for Alloy Fuels

## ASME 2010

Changhu Xing
ColbyJensen
Heng Ban
Robert Mariani
J. Rory Kennedy

November 2010

ASME 2010 International Mechanical Engineering Congress and Exposition

IMECE
November 12-18, 2010, Vancouver, British Columbia, Canada

IMECE2010-39457

# AN ELECTROMOTIVE FORCE MEASUREMENT SYSTEM FOR ALLOY FUELS

**Changhu Xing, Colby Jensen, Heng Ban**
Mechanical and Aerospace Engineering,
Utah State University, 4130 Old Main Hill,
Logan, UT 84322

**Robert Mariani, and J. Rory Kennedy**
DOE Idaho National Lab,
Idaho Falls, ID 83415

## ABSTRACT

The development of advanced nuclear fuels requires a better understanding of the transmutation and micro-structural evolution of the materials. Alloy fuels have the advantage of high thermal conductivity and improved characteristics in fuel-cladding chemical reaction. However, information on thermodynamic and thermophysical properties is limited. The objective of this project is to design and build an experimental system to measure the thermodynamic properties of solid materials from which the understanding of their phase change can be determined. The apparatus was used to measure the electromotive force (EMF) of several materials in order to calibrate and test the system. The EMF of chromel was measured from 100°C to 800°C and compared with theoretical values. Additionally, the EMF measurement of Ni-Fe alloy was performed and compared with the Ni-Fe phase diagram. The prototype system is to be modified eventually and used in a radioactive hot-cell in the future.

## INTRODUCTION

The Fuel Cycle Research & Development programs propose, in part, to transmute highly radioactive and long lived transuranic (TRU) isotopes so as to close the nuclear fuel cycle and reduce the volume, heat load, and radiotoxic burden of the deep geological repository at Yucca Mountain. Key to the implementation of these programs is an understanding of the performance and behavior of transmuted nuclear fuels, mainly, the material structure of the alloy fuels. Many experimental techniques can be used to determine the thermodynamic quantities of a material such as calorimetric measurement, gas phase equilibrium techniques and Electromotive force (EMF) measurement method [1]. Among these methods, the EMF measurement technique has its unique advantages. When a thermal cell is built, it involves a direct measurement of thermal EMF and Seebeck coefficient/thermopower/thermoelectric power of a sample material when it is contacted with a reference conductor whose thermoelectric properties have been determined. When a sample material undergoes a pressure induced or temperature led phase transformation, both its structural and electronic properties will change correspondingly. At a temperature and pressure combination where a phase transition takes place, both the chemical potential and Fermi energy will undergo a discontinuity which causes a change in thermopower [2-6]. Thus, the Seebeck coefficient generally presents an anomalous behavior in the form of abrupt variation corresponding to the change of material structure.

Based on the characteristics of the thermal EMF of a material with relation to its material structure, an experimental system was designed and built for the determination of its thermodynamic properties. A calibration of the system was performed with respect to chromel wire, one of the legs of type K thermocouple without a phase transition and an iron-nickel alloy, with phase change present in its solid state. The measurement system will be adapted to the determination of material structure of alloy fuels at a later stage.

## MEASUREMENT PRINCIPLE

When two dissimilar metals are connected with a temperature difference existing at the two separate junctions, an electric potential is generated in the circuit. The Seebeck voltage depends only on the two dissimilar materials and the temperature difference present at their junctions. Thus for the selected materials, the Seebeck coefficient can be written as

$$S = -\frac{\Delta V}{\Delta T} \tag{1}$$

Where ΔV is the EMF and ΔT is temperature difference. When ΔT approaches zero, the difference becomes differentiation

$$S = -\lim_{\Delta T \to 0} \frac{\Delta V}{\Delta T} = -\frac{dV}{dT} \tag{2}$$

Figure 1 presents an illustration of the configuration of thermopower determination [7]. This technique determines a sample EMF and thermopower in comparison with a reference material.

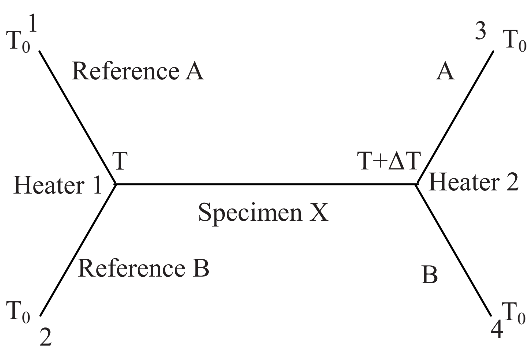


Fig. 1 Schematic arrangement of the thermopower measurement

A specimen of material X is placed in a furnace with its two ends welded to two thermocouples. The materials of the thermocouple wires are A (leads 1, 3) and B (leads 2, 4). Micro-heater(s) is/are attached to one side or both sides of the specimen to generate a temperature difference ΔT across the specimen. The temperature values at the two ends are measured through the thermocouple leads 1, 2 at the cold side and 3, 4 at the hot side. At the same time, an electrical potential difference ΔV is generated through the circuit A-X-A due to the Seebeck effect and measured from leads 1, 2. Any thermocouple may be used for the temperature measurement but the material of wire A needs to have a known and stable absolute thermopower.

For a circuit comprised of A-X-A (1-X-3), the measured thermopower is a contribution from both A and X.

$$\Delta V_{X,A} = (S_A - S_X)\Delta T$$
$$\Rightarrow S_X = S_A - \Delta V_{X,A} / \Delta T \tag{3}$$

Where $\Delta V_{X,A}$ is the measured EMF in the experiment, $S_A$ is the Seebeck coefficient of reference A and $S_X$ is the Seebeck coefficient of specimen X. In general, the temperature difference ΔT is calculated by the subtraction of the temperature values at the two junctions. In addition, when the thermopower for the reference material A is known, the thermopower for the test sample can be obtained at the mean temperature of the sample, T+ΔT/2.

Two methods are generally used in thermopower measurement experiments. The first procedure is that while holding one junction of the circuit in a constant temperature bath, the temperature at the second junction is raised gradually and the corresponding EMFs are measured over the temperature range. The thermopower is then obtained by differentiating the electromotive force versus temperature curve. This method is good for materials with a wire shape. The second scheme is that while heating up the two junctions to the required temperature, an additional increase of ΔT is made at one junction. The thermopower can be obtained by measuring the change of EMF corresponding to the temperature difference. The 2nd scheme is adopted in this experiment due to the rod shape of the sample.

Since thermopower of the reference thermocouples is needed in Eq. (3), it is necessary to obtain an expression of the Seebeck coefficient with respect to temperature. Most of the material thermopower is measured based on platinum. Thus, manipulation of absolute thermopower of platinum and EMF of thermoelements relative to platinum is necessary [8-10]. Figure 2 presents a plot of the absolute thermopowers of type K and type N thermoelements and platinum, which will be used as reference values in the measurement.

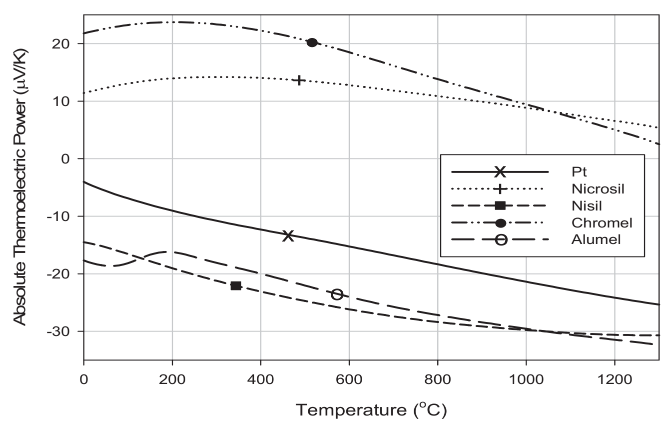


Fig. 2 Absolute Thermoelectric power of platinum, nicrosil, nisil, chromel and alumel

## EXPERIMENTAL METHODS

Figure 3 presents a schematic illustration of the instrument employed in the experiment. The whole experimental system includes a heating unit (MTI OTF-1200X horizontal tube furnace), temperature control unit, atmospheric control unit and data acquisition unit. As illustrated in the figure, when the test section was inserted into the furnace, the support system, thermocouple wires and power cords were led out of the high temperature region to pass through plugs installed in the gas tight gaskets on the four-way cross. The temperature control unit includes a Eurotherm 3504 controller and TDK-Lambda power supply. A program was written in the controller to control the power input to maintain a specified temperature in the test section. A vacuum pump was used to create a vacuum environment and flowing, high purity helium was employed to reduce oxidation and contact resistance between the sample and heater as well as the sample and heat sink. An Agilent 34970 data acquisition (DAQ) unit and computer were used for monitoring and recording the temperature and EMF data.

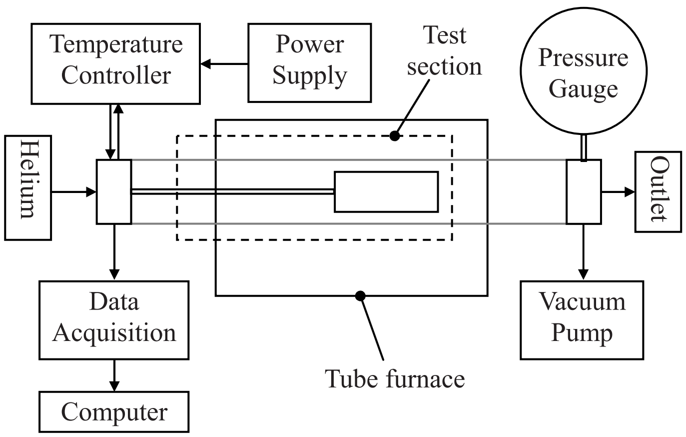


Fig. 3 Schematic illustration of instrumentation

A piece of chromel wire approximately 50.8 mm (2") long with a diameter of AWG 20 (0.032") was used as the sample for the first measurement. Based on Figure 1, two type-N thermocouples with a diameter of AWG 30 (0.01") were welded at the two ends of the chromel wire. All of the thermoelements used in the experiment were purchased from Omega and according to the specifications given in [11], sizes AWG 20 and 30 of both type K and N thermocouples have an upper temperature limit of 980 $^{o}$C and 870 $^{o}$C respectively. Nextel 312 sleeving is used to insulate each wire strand. The tube furnace was employed to vary the working temperature. In order to test an appropriate temperature difference range, the chromel system was heated by the furnace alone and a temperature difference across the two ends was generated by the natural temperature distribution of the tube furnace. The parabolic temperature distribution inside the furnace was calibrated by a special limit type N thermocouple.

The second tested specimen is made of an iron-nickel alloy. The alloy rod has a composition of 15 wt% of nickel and a diameter of 12.7 mm (0.5"). It was purchased from ESPI metals with a purity of 99.99%. The arrangement of the test section is illustrated in Figure 4 where a total of six thermocouples were used. Two type N thermocouples (5 and 6) were connected to the controller where a fixed temperature difference of 5 $^{o}$C was applied; two type N thermocouples (3 and 4) and two type S thermocouples (1 and 2) were connected to the data acquisition system. While the temperature data was being acquired by the DAQ, the voltage differences from type S (1+ vs. 2+ and 1- vs. 2-) thermoelements and type N (3+ vs. 4+ and 3- vs. 4-) themoelements were detected by the DAQ as well. The employment of both type N and type S thermocouples is used to validate each other.

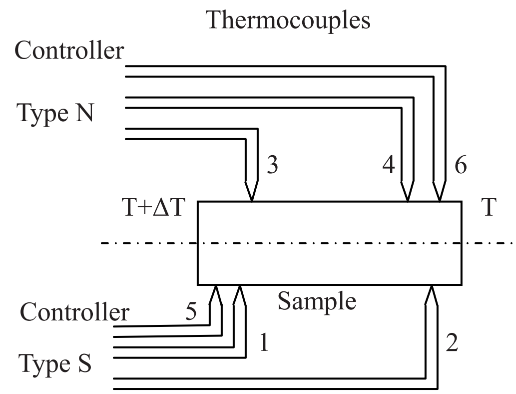


Fig.4 Schematic arrangement of the thermopower measurement for iron-nickel alloy

Different from the chromel measurement, a micro resistance heater is contacted with the sample on one end and a heat sink on the other. The whole test section is wrapped by insulation material thus leaving thermal conduction mechanism only in the heat transfer process. The amount of power needed for keeping a constant temperature difference at different furnace temperatures was controlled by the controller. Before the measurement was carried out in the system, the vacuum pump was used to reduce the pressure inside the quartz tube and then helium was backfilled into the tube. An inert gas environment pressurized to 25.7mm (1") water was maintained throughout the whole test.

During the initial stage, the specimens were at room temperature (around 22 $^{o}$C). The furnace temperature was increased slowly to 750 $^{o}$C with a heating rate around 0.75 $^{o}$C/min. The temperature and thermal potential were collected at a sampling rate of 0.1 sample per second. The temperature was maintained at 750 $^{o}$C for two hours followed by a cooling process performed at a similar cooling rate of -0.75 $^{o}$C/min down to room temperature. Thus the EMF is measured in a quasi-static way.

## RESULTS AND DISCUSSIONS

Figure 5a presents the measured thermopower variation of chromel with the change of temperature. The absolute thermopower was obtained by solving Eq. (3). As a comparison, the corresponding theoretical value based on Figure 2 is superimposed on the same figure. The temperature difference varied from 5 $^{o}$C to 30 $^{o}$C but most of the time, centered at a range of 10-20 $^{o}$C. From this figure one can see that the measured values closely followed the theoretical ones even with such large $\Delta T$. Figure 5b presented the deviation from the measured and reference values from which it showed that the deviation is mostly within 3%. The deviation may be caused by the error of the thermocouple which is 2.2 $^{o}$C or 0.75% of reading or due to the quasi-static measurement. Another fact that may be reviewed is that the deviation in the cooling process is always slightly higher than that in the heating process. This may be caused by thermocouple de-calibration which is the result of contamination and thermal EMF drift when the thermocouples were exposed at high temperature too long. Another factor contributing to the deviation is the uncertainty and resolution of the DAQ. With the minimum voltage range of ±100 mV and a resolution of 6.5 digits, the voltage resolution is 0.05 μV. For an accuracy of ±0.004% of reading + ±0.004% of range, the uncertainty is around ±4 μV.

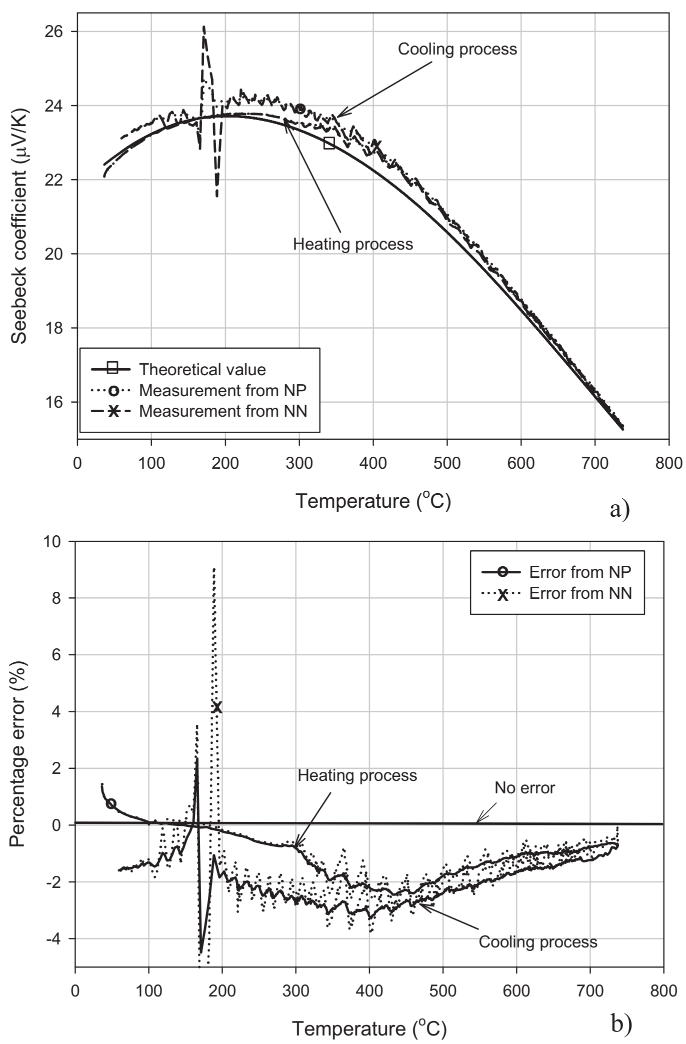


Fig. 5 Measured, literature Seebeck coefficients and the deviation with respect to temperature a) absolute thermoelectric power b) deviation

When a temperature difference (5 $^{o}$C) was adopted by the controller, the temperature dependent EMF of iron-15 wt% nickel alloy was measured according to Figure 4. A review of the Fe-Ni phase diagram [12] indicates that at room temperature, this alloy rod is comprised of a combination of αFe,Ni + $FeNi_3$ (see Figure 6). At a composition of 50.6 wt% of nickel, the two-phase mixture becomes completely γFe,Ni through a eutectoid transformation at 347 $^{o}$C. However, for a composition of 15 wt% of nickel, the combination transforms to αFe,Ni + γFe,Ni through a hypo-eutectoid transformation. Above 658 $^{o}$C until its solidus temperature, γFe,Ni exists as a single solid phase. Therefore, from the equilibrium phase diagram, this alloy would undergo two phase transitions in the temperature range from 0 to 750 $^{o}$C. At low temperatures (<800 $^{o}$C), diffusion is very low and consequently, the phase transition time required is very long. The eutectoid temperature is especially not easy to find. For instance, in his EMF measurement (Figure 6), Tanji [4] detected the solvus temperature around 635 $^{o}$C but detected no indication regarding the eutectoid temperature. The EMF measurement in the Tanji experiment adopted the integration scheme mentioned above and the thermopowers presented in his figures are values relative to platinum.

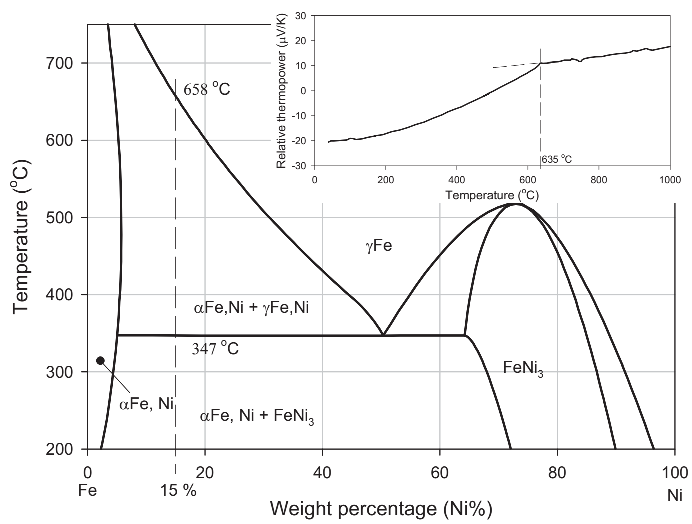


Fig. 6 Illustration of the studied alloy on the equilibrium phase diagram and measurement by Tanji

Figure 7 presents the measured absolute thermopower of Fe-Ni alloy during heating and cooling processes. The results from type N and type S thermocouples had some difference at temperatures below 300 $^{o}$C during the heating process. During the cooling process, the type N thermocouple detached from the sample below 430 $^{o}$C but the result from the type S thermocouple was still a good indicator revealing its structure variation. In the heating process, the Seebeck coefficient varied slowly with temperature change initially. However, the slope changed drastically around 306 $^{o}$C from the type S and 317 $^{o}$C from the type N measurement, which indicated that the alloy structure changed. The measured temperature, although slightly different from the equilibrium eutectoid temperature, is still a good sign for this measurement technique in that the structure change was grasped at such a low temperature in the current experiment.

Above the transition temperature, both the measured Seebeck coefficients from type N and S increased with temperature in a similar rate until they hit another transition temperature. Sharing the same curve type and legend as Figure 7a, Figure 7b presents a blowup of the values from 590-740 $^{o}$C where one can see that the measured transition temperature from the type N is around 609 $^{o}$C during heating process. However, this temperature was measured to be 630 $^{o}$C during cooling stage. From the type S thermocouple, it can be observed that the measured values were both around 630 $^{o}$C. A comparison between these measured values with ones from literature indicates that they are very close. The measured value was 630 $^{o}$C while the Tanji temperature was 635 $^{o}$C and the equilibrium temperature is around 658 $^{o}$C. Another point that can be seen is that the measured values from type N thermocouples varied largely above 600 $^{o}$C while results from type S thermocouples were pretty consistent. Similar to Figure 5, this may be due to the de-calibration of thermocouples although the maximum allowable temperature is 870 $^{o}$C.

During the cooling process, the measured thermopower deviates from the one in the heating process significantly. Thus the structure of the alloy rod is not only determined by the temperature but also its heating history, the thermal lag of the instrument, and potentially differing kinetic rates for the forward and reverse reactions. In the γFe,Ni temperature zone, the holding time for the specimen temperature may not be long enough to transform its structure completely. For example, during the cooling process at a given temperature, the percentage of mixed phases may not be the same as the one in the heating process for the same temperature. A much lower eutectoid temperature, around 200 $^{o}$C, is observed in the cooling process and this may be the complete transformation temperature. At the conclusion of the run, the structure of the specimen changed back to its original state as reflected by the measured thermopower, which agreed with the initial measurement.

## CONCLUSIONS

An experimental system was designed and built for the measurement of thermal electromotive force varying with temperature of a specimen. Its temperature dependent, absolute thermopower was determined by considering theoretical values of the reference measuring elements. By calibrating the system with a measurement of chromel, it was found that the deviation is within 3%. When a phase-transition iron-nickel alloy was measured, the abrupt EMF change clearly indicated phase transformations at certain temperatures. The measured $\alpha + \gamma$ to $\gamma$ transition temperature was close to the equilibrium value and one obtained in a reference. In addition, the eutectoid transition was observed in this measurement.

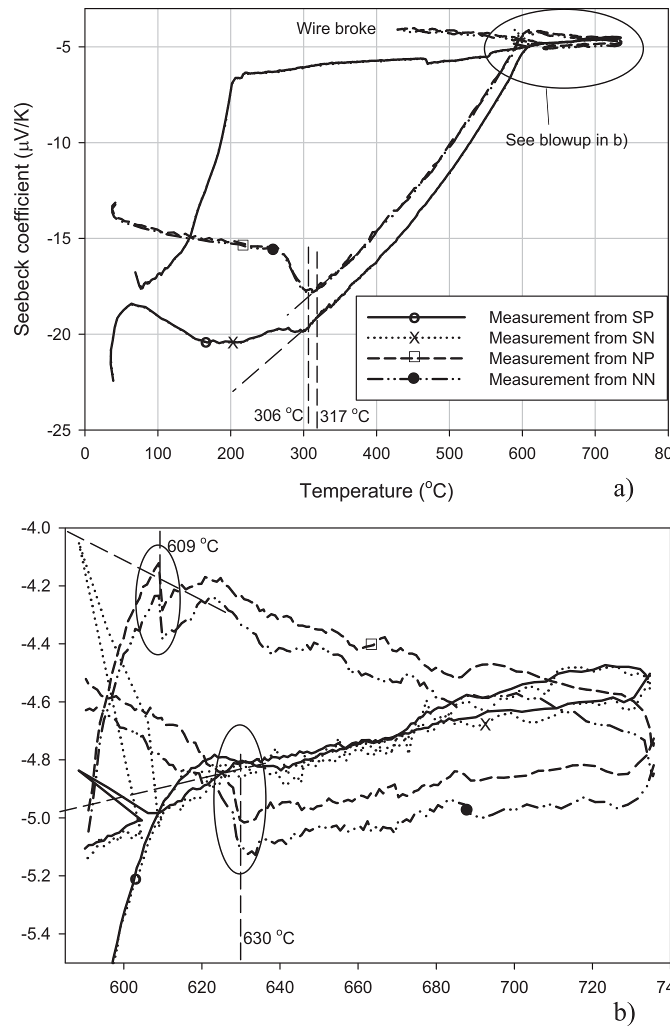


Fig. 7. Measured absolute thermopower of Fe- 15 wt% Ni alloy with respect to temperature a) absolute thermopower b) blowup of circled curve in a)

## REFERENCES


[1] Saunders, N., Miosoqnik, A. P., 1998, CALPHAD (Calculation of Phase Diagrams)-A Comprehensive Guide, Pergamon, New York.

[2] Pollock, D. D., 1985, Thermoelectricity: Theory, Thermometry, Tool, American Society for Testing & Materials, Philadelphia.

[3] Tani, T., Tanaka, S., 1984, "Thermoelectric Power Observation of Nearly-Commensurate Charge-Density Wave Phase in 1T-TaS2," J. Phys. Soc. Jpn. , 53(5), pp. 1790-1796.

[4] Tanji, Y. M., H., Nakagawa, Y., 1978, "Anomalous Concentration Dependence of Thermoelectric Power of Fe-Ni (fcc) Alloys at High Temperatures," J. Phys. Soc. Jpn., 45(4), pp. 1244-1248.

[5] Ramesh, T. G., Shubha, V., 1994, "Thermopower and Resistivity in the Study of Continuous Phase Transitions," Proceedings of the National Conference on High Pressure Science and Technology, Bangalore, India, pp. 65-74.
[6] Ovsyannikov, S. V., Shchennikov,V. V., 2004, "Phase Transitions Investigation in ZnTe by Thermoelectric Power Measurements at High Pressure " Solid State Commun., 132(5), pp. 333-336.
[7] Barnard, R. D., 1972, Thermoelectricity in Metals and Alloys, Taylor & Francis Group, New York.
[8] ASTM, 2003, "Standard Specification and Temperature-Electromotive Force (EMF) Tables for Standardized Thermocouples."
[9] Causack, N., Kendall, P., 1958, "The Absolute Scale of Thermoelectric Power at High Temperature," Proc. Phys. Soc., 72(5), pp. 898-901.
[10] Roberts, R. B., Righini, F., Compton, R. C., 1985, "Absolute Scale of Thermoelectricity III," Philos. Mag. B, 52(6), pp. 1147-1163.
[11] Omega, 2007, Omega Temperature Measurement Handbook, Omega Engineering Inc.
[12] Swartzendruber, L. J., Itkin, V. P., Alcock, C. B., 1991, "The Fe-Ni (Iron-Nickel) System," J. Phase Equilib., 12(3), pp. 288-312.